

# Magnetic and structural characterization of thiol capped ferromagnetic Ag nanoparticles

E. Goikolea,<sup>1</sup> J. S. Garitaonandia,<sup>1,a)</sup> M. Insausti,<sup>1</sup> I. Gil de Muro,<sup>1</sup> M. Suzuki,<sup>2</sup> T. Uruga,<sup>2</sup> H. Tanida,<sup>2</sup> K. Suzuki,<sup>3</sup> D. Ortega,<sup>4</sup> F. Plazaola,<sup>1</sup> and T. Rojo<sup>1</sup>

<sup>1</sup>*Zientzia eta Teknologia Fakultatea, Euskal Herriko Unibertsitatea, 644 pk, E-48080 Bilbao, Spain*

<sup>2</sup>*Japan Synchrotron Radiation Research Institute/SPring-8, 1-1-1 Kouto, Sayo, Hyogo 679-5198, Japan*

<sup>3</sup>*Department of Materials Engineering, Monash University, Clayton, VIC 3800, Australia*

<sup>4</sup>*The Davy-Faraday Research Laboratory, 21 Albemarle Street London W1S 4BS, United Kingdom*

(Presented 19 January 2010; received 9 November 2009; accepted 12 January 2010; published online 13 May 2010)

Dodecanethiol capped Ag nanoparticles (NPs) have been independently synthesized by the well-known Brust method under the same physical-chemical conditions. The obtained NP present similar sizes ( $\sim 2$  nm) but different magnetic behaviors. The extended x-ray absorption fine structure analyses at the  $K$ -edge of Ag did not reveal any noticeable structural nor topological differences among the samples. In clear contrast with the structure provided for thiol capped ferromagnetic Au NPs, the analysis also brings out the existence of Ag-S bonds in a diffuse region surrounding a reduced Ag core where the magnetism of the Ag NPs would be located. © 2010 American Institute of Physics. [doi:10.1063/1.3367978]

## I. INTRODUCTION

The appearance of ferromagnetism at nanoscale in materials which are nonmagnetic at bulk state is intimately related to local changes arranged in the electronic structure of the material. At these sizes the number of atoms forming the structure of the nanoparticle (NP) is limited and, thus, the local electronic unbalance generated by defects or foreign elements become significant when the total energy is minimized to stabilize the NP. The final profile of the electronic structure turns up remarkably modified, leading to enough local energy to maintain the magnetic moments directionally fixed even at room temperature (RT). Proton irradiated graphite, doped ZnO, or Pd NPs can be mentioned as examples of materials where this ferromagnetism has been induced.<sup>1-3</sup> Ferromagnetism can be also induced by varying the chemical and physical conditions of the atoms at the surface of a NP. Surface atoms show broken symmetries and they are exposed to the presence of external agents such as chemical cappings. As in a nanometer scale the relative quantity of surface atoms is comparable and even higher than the quantity of atoms in the interior of the NP, the contribution of the surface atoms to the final electronic structure of the NP is the dominant one and any change at the surface of the NP will be immediately reflected in changes in its electronic structure. In thiol capped ferromagnetic NPs, the interaction among the S atoms of the thiols and the surface atoms of the NPs induces a charge transfer from the bonded atoms, generating spin imbalances in the surface atoms. These spin imbalances can house different anisotropies, giving rise to different magnetic characters including superparamagnetism down to 2 K and ferromagnetism at RT.<sup>4-9</sup>

Although the samples can be of different chemical nature, this induced permanent ferromagnetism presents in most of the cases common characteristics such as coercive

field or small dependence of the saturation magnetization with the temperature, suggesting that the underlying mechanisms of magnetism can be similar. In this paper we compare and analyze electron x-ray absorption fine structure (EXAFS) of thiol capped Ag NPs with different magnetic behaviors. The results are also contrasted with the EXAFS of a ferromagnetic thiol capped Au NPs.

## II. EXPERIMENTAL PROCEDURES

Dodecanethiol capped Ag NPs (Ag-SR NPs) were synthesized by a modification of the so-known Brust method. The details of synthesizing process have been described elsewhere.<sup>8</sup> Transmission electron microscope (TEM) images were obtained by a TEM Philips CM200. Macroscopic magnetization measurements were obtained by a superconducting quantum interference device magnetometer (Quantum Design). The EXAFS spectra were recorded in transmission mode at RT at the beamline BL01B1 of SPring-8 synchrotron radiation facility. The spectra were fitted to the standard EXAFS equation using ARTEMIS program.<sup>10</sup> The obtained samples were divided in different groups depending of their magnetic signal. In this work we present the results of representative samples of these groups.

## III. RESULTS AND DISCUSSION

Figure 1 shows the TEM micrographs and particle size distribution histograms of three dodecanethiol capped Ag NPs. All the synthesized samples exhibit similar structural features. They commonly show the fcc crystal structure of the metallic Ag, narrow size distributions, and average particle sizes slightly higher than 2 nm.  $M(H)$  curves of these samples are shown in Fig. 2. The sample labeled as Ag-SR1 shows a predominant diamagnetic behavior down to 5 K whereas the samples Ag-SR2 and Ag-SR3 show a clear ferromagnetic behavior even at 300 K.

<sup>a)</sup>Electronic mail: js.garitaonandia@ehu.es.

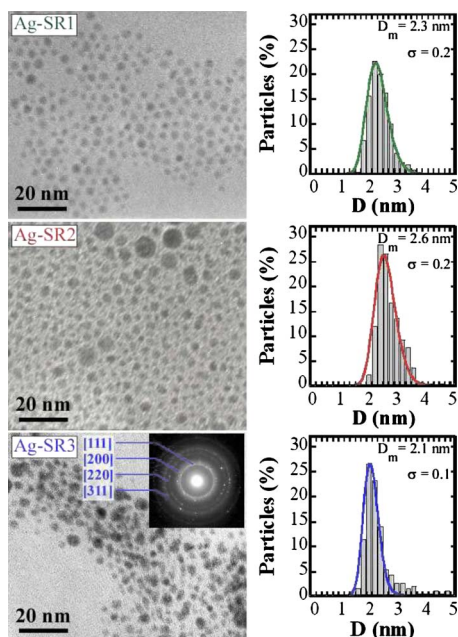


FIG. 1. (Color online) TEM images of studied dodecanethiol-capped Ag NPs and their corresponding size distributions histograms. The solid line represents the fitting curve assuming a log-normal function. The calculated average particle diameter  $D_m$  and the standard deviation  $\sigma$  are shown in the histograms. Electron diffraction patterns for Ag-SR3 sample are shown in the inset.

We have completed the structural characterization of the Ag-SR1 (diamagnetic) and Ag-SR2 (ferromagnetic) labeled Ag NPs by analyzing the normalized EXAFS spectra obtained at the  $K$ -edge of Ag. Figure 3 shows the EXAFS spectra of the samples together with the spectrum of a Ag foil. The spectra corresponding to the Ag NPs present very similar fine structures composed of oscillations of lower intensity as compared with those observed in the spectrum of the Ag foil. This feature is commonly observed in the absorption spectra of systems with reduced number of atoms. However, despite the fcc crystal structure observed by TEM, the maxima and the minima of these oscillations do not fit with the fine structure of the spectrum of the Ag foil which clearly reflects the influence of the Ag atoms bonded to the S atoms of the dodecanethiol on the electronic structure of the whole

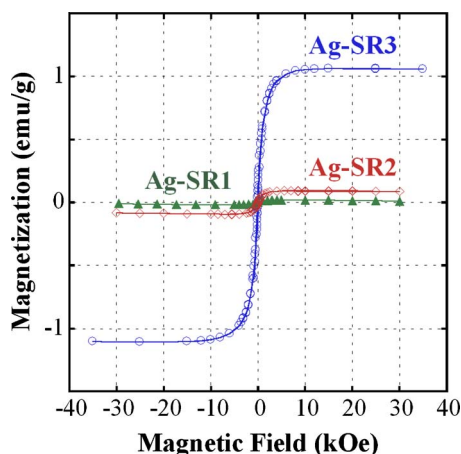


FIG. 2. (Color online) Magnetization curve obtained at 5 K for Ag-SR1 sample and magnetization curves obtained at 300 K for Ag-SR2 and Ag-SR3 samples.

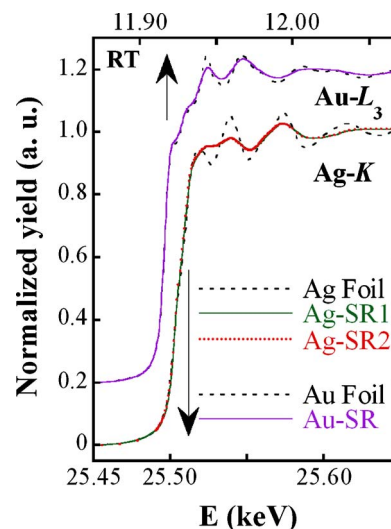


FIG. 3. (Color online) Ag  $K$ -EXAFS spectra for samples Ag-SR1, Ag-SR2, and a Ag foil together with Au  $L_3$ -EXAFS spectra obtained for previously reported ferromagnetic Au-thiol NPs.

NP. In Fig. 4(a) we show the radial distribution functions obtained after the Fourier transformation of the EXAFS region over the  $k$ -range of  $2$ – $10$   $\text{\AA}^{-1}$  (not corrected for the phase shift). The results in both diamagnetic Ag-SR1 and ferromagnetic Ag-SR2 samples show that the distances and coordination numbers are, respectively,  $\sim 2.9$   $\text{\AA}$  and  $\sim 3.4$  for Ag–Ag and  $\sim 2.4$   $\text{\AA}$  and  $\sim 1.3$  for Ag–S, reflecting the structural and topological similarities of both samples. With the aim of contrasting the results of Ag NPs with their Au counterparts, in Fig. 3 we have added the EXAFS spectra obtained at the  $L_3$ -edge of a Au foil and of a ferromagnetic thiol Au NPs (sample Au-SR2 in Ref. 12) with an average size of  $\sim 2.2$  nm, similar to those estimated for the Ag NPs presented in this work. The radial distribution function obtained after the Fourier transformation of the corresponding EXAFS region [Fig. 4(b)] offers distances and coordination numbers of  $\sim 2.8$   $\text{\AA}$  and  $\sim 4.8$  for Au–Au and  $\sim 2.5$   $\text{\AA}$  and  $\sim 0.9$  for Au–S, respectively. Therefore, there is a consistency among the calculated distances in both Au and Ag NPs but a notable discrepancy with regard to the coordination numbers.

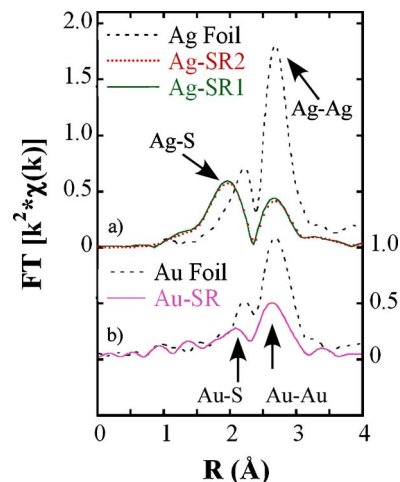


FIG. 4. (Color online) (a) Fourier transform of the EXAFS signal ( $K$ -edge) of Ag-SR1 and Ag-SR2 samples and Ag foil (dashed line) and (b) of the EXAFS signal ( $L_3$ -edge) of Au-SR2 sample and Au foil (dashed line).

An alternative image of the Ag NPs can be drawn based on the structural information extracted from the EXAFS spectra. In a simple NP model composed of shells of fcc structured Ag atoms, the above EXAFS results would lead to a scenario where less than 10% of the total Ag atoms are exclusively surrounded by Ag atoms. This would limit the NPs to only one Ag shell cluster and a size of less than the half of the average sizes evaluated from TEM images. The same calculation for the Au sample would lead to a NP formed by two shells of fcc structured Au atoms with  $\sim 76\%$  of the Au atoms located at the surface of the NP, whereas the relative quantity of surface atoms calculated for a Au or Ag NP with an average size of  $\sim 2.2$  nm would decrease down to 52%. In the case of the Au sample the difference between the relative quantity of surface atoms calculated from EXAFS data and from TEM micrographs (76% and 52%) can be overcome if deviations of the morphology of the NPs from a model of perfectly fcc structured shells are taken into account. It has been observed that in the 1–3 nm range Au NPs present exclusively icosahedral and decahedral morphologies with remarkably higher surface to inner atoms ratio than a quasi spherical fcc shell structured NP with the same size.<sup>11</sup> In addition, the possible presence of residual side products formed during the synthetic procedure such as dimmers, trimers, and smaller clusters would also contribute to slightly divert the calculated coordination numbers to smaller values than the expected ones. However, in the case of the Ag NPs the large difference between the two figures ( $>90\%$  and 52%) cannot be justified simply by the possible morphological difference or by a low yield of the chemical synthesis. This rather large discrepancy in the ratio between the number of atoms in the core part and the surface suggests strongly that not only the Ag atoms on the surface monolayer but also the Ag atoms of inner layers of the NPs are linked to the S atoms of the capping compound. Hence, the boundary between the pure metallic Ag NPs and external capping could be diffuse.

The near-edge structure region of the XAS spectra of thiol capped Au NPs at  $L_3$ -edge show higher intensities in the first resonance at the threshold (white line) when are compared to that for the Au foil, revealing that the density of the 5d states is reduced in the Au NPs as consequence of a charge transfer to the S atoms.<sup>12</sup> In a generally accepted explanation, magnetism in Au NPs is located in the so generated unoccupied densities of d states.<sup>4</sup> However, although the magnetic character of these d states has been confirmed,<sup>8</sup> it has been also observed that there is not a linear relation among relative 5d charge transfer and magnetism. Furthermore, 5d electron transfer does not guarantee the apparition of magnetism in Au NPs.<sup>13</sup> Magnetism in thiol capped NPs has been associated to a very determinate arrangement of the electronic states of the surface bonded atoms, being this arrangement hidden in the measured x-ray appearance near-edge structure by overlapping with the signal from the atoms of the core of the NP.<sup>9</sup> A comparison of the relative intensity of the magnetic contribution of a Mössbauer spectrum performed on ferromagnetic thiol capped Au NPs with their average particle size obtained by TEM allowed us to con-

firm experimentally the apparent limitation of the magnetism to the surface Au atoms.<sup>8</sup> The results obtained from the EXAFS spectra of the analyzed Ag NPs lead to two different conclusions. (a) The Ag NPs studied in this work were independently synthesized under the same chemical-physical conditions and using the same chemical precursors. Independently of their magnetic character, the samples show similar sizes, structures, and topologies. The precise chemical and structural keys determining the apparition or not of ferromagnetism are yet to be established. (b) From a qualitative point of view, the Ag NPs are composed of a core of fcc structured Ag atoms surrounded by compositionally undefined layers of Ag atoms bonded to the S atoms of the dodecanethiol. This possibility has been also suggested for thiol capped ferromagnetic NPs.<sup>14</sup> Taking into account the location of magnetism on the surface Au atoms in Au magnetic NPs, the magnetism in Ag ferromagnetic NPs would be expected to be located in the Ag atoms of this transitional region. This is an important aspect since, if it is confirmed, the magnetism of these NPs would place also out of the surface of the metallic core.

## ACKNOWLEDGMENTS

Financial support from the Spanish CICYT CICYT and Basque Government under Grant Nos. MAT2009-14398, MAT2007-66737-C02-01, IT-382-07, and SAIOTEK-SPE08UN80 and by Australian Research Council. E.G. thanks the Basque Government for financial support. The EXAFS experiments at Spring-8 were performed with the approval of the JASRI (Proposal No. 2008A1567).

<sup>1</sup>P. Esquinazi, D. Spemann, R. Höhne, A. Stter, K. H. Han, and T. Butz, *Phys. Rev. Lett.* **91**, 227201 (2003).

<sup>2</sup>S. J. Chen, K. Suzuki, and J. S. Garitaonandia, *Appl. Phys. Lett.* **95**, 172507 (2009).

<sup>3</sup>T. Taniyama, E. Ohta, and T. Sato, *Europhys. Lett.* **38**, 195 (1997).

<sup>4</sup>Y. Yamamoto, T. Miura, M. Suzuki, N. Kawamura, H. Miyagawa, T. Nakamura, K. Kobayashi, T. Teranishi, and H. Hori, *Phys. Rev. Lett.* **93**, 116801 (2004).

<sup>5</sup>P. Crespo, R. Litrán, T. C. Rojas, M. Multigner, J. M. de la Fuente, J. C. Sánchez-López, M. A. García, A. Hernando, S. Penadés, and A. Fernández, *Phys. Rev. Lett.* **93**, 087204 (2004).

<sup>6</sup>R. Litrán, B. Sampedro, T. C. Rojas, M. Multigner, J. C. Sánchez-López, P. Crespo, C. López-Cartes, M. A. García, A. Hernando, and A. Fernández, *Phys. Rev. B* **73**, 054404 (2006).

<sup>7</sup>L. Suber, D. Fiorani, G. Scavia, and P. Imperatori, *Chem. Mater.* **19**, 1509 (2007).

<sup>8</sup>J. S. Garitaonandia, M. Insausti, E. Goikolea, M. Suzuki, J. D. Cashion, N. Kawamura, H. Ohsawa, I. Gil de Muro, K. Suzuki, F. Plazaola, and T. Rojo, *Nano Letters* **8**, 661 (2008).

<sup>9</sup>M. A. García, J. M. Merino, E. Fernández Pinel, A. Quesada, J. De la Venta, M. L. Ruiz González, G. R. Castro, P. Crespo, J. Llopis, J. M. González-Calvet, and A. Hernando, *Nano Lett.* **7**, 1489 (2007).

<sup>10</sup>B. Ravel and M. Newville, *J. Synchrotron Radiat.* **12**, 537 (2005); B. Ravel, M. Newville, D. Haskel, J. J. Rehr, E. A. Stern and Y. Yacoby, *Physica B* **208**, 154 (1995).

<sup>11</sup>C. L. Cleveland, U. Landman, T. G. Schaaff, M. N. Shafigullin, P. W. Stephens, and R. L. Whetten, *Phys. Rev. Lett.* **79**, 1873 (1997).

<sup>12</sup>P. Zhang and T. K. Sham, *Phys. Rev. Lett.* **90**, 245502 (2003).

<sup>13</sup>J. S. Garitaonandia, E. Goikolea, M. Insausti, M. Suzuki, N. Kawamura, H. Ohsawa, I. Gil de Muro, K. Suzuki, J. D. Cashion, C. Gorria, F. Plazaola, and T. Rojo, *J. Appl. Phys.* **105**, 07A907 (2009).

<sup>14</sup>C. López-Cartes, T. C. Rojas, R. Litrán, D. Martínez-Martínez, J. M. de la Fuente, S. Penadés, and A. Fernández, *J. Phys. Chem. B* **109**, 8761 (2005).